WAVELET FILTERING OF SAR IMAGES BASED ON NON GAUSSIAN ASSUMPTIONS

Samuel Foucher[1], *Goze B. Bénié*[1], *Jean-Marc Boucher*[2]

[1]CARTEL, Université de Sherbrooke, Sherbrooke, Québec, Canada
e-mail: sfoucher@callisto.si.usherb.ca
[2]ENSTB, Brest, France

ABSTRACT

Radar images are affected by a multiplicative noise depending on the underlying signal (the ground reflectivity) due to the coherence of the radar wavelength. Images present a strong pixel to pixel variability considerably reducing the efficiency of target detection and classification algorithms. We propose in this study filtering this noise using image multiresolution analysis. The value of the wavelet coefficients of the radar reflectance is estimated by a Bayesian model by maximizing the a posteriori density and by modeling the different densities using the Pearson distributions system. The resulting filter combines a classical adaptive approach and wavelet decomposItion using the local variance of the wavelet coefficients for segmenting and weighting the latter taking into account the multiplicative nature of the noise.

1. INTRODUCTION

The advent of synthetic aperture radars has resulted in marked improvements in the spatial resolution of images. The nominal resolutions are now available below ten meters. Nevertheless, the radiometric resolution of the ground targets is heavily degraded by the presence of a multiplicative noise, typical of coherent imagery, labeled as speckle noise. This results in an important reduction in the efficiency of classification and target detection algorithms. In order to improve the radiometric resolution, images generally undergo a multiview processing during the formation stage of the images by the processor. Hence, the averaging of L views of the same scene permits the reduction of the gray level variance of a homogeneous target by a factor L. Unfortunately, this radiometric improvement is accompanied by a loss in resolution of the same magnitude. Consequently, high resolution SAR images are characterized by a low number of views which require the application of filtering techniques.

Since the 8o's, the techniques of speckle reduction have known considerable development. To the first heuristic filters (median filters, Crimmins filter, etc) have succeeded adaptive filters taking into account the local information content. Most of the adaptive filters start from the consequences of the multiplicative model for segmenting the image into homogeneous and heterogeneous zones using the local normalized standard deviation. Over the heterogeneous zones, the ground reflectivity can be estimated by a simple local mean. The different filters differ by the filtering of the heterogeneous zones; for instance the Lee [1] and Kuan filters use a local MEQM criteria [2]. More recently, the Gamma -MAP filter starts from well established models for the speckle and reflectivity probability density functions (pdf). The application of a Maximum A Posteriori (MAP) criteria leads to an estimation of the reflectivity as a solution of a second degree equation [3].

The method proposed here starts from a wavelet representation of the image. The objective is to filter the wavelet coefficients obtained by suppressing the nosiy ones and weighting those engendered by significant structures of the image. A few attempts were made at filtering of SAR images by wavelet, essentially by filtering the wavelet decomposition of the logarithm of the image gray levels [4]. The problem of filtering can be reduced hence to the case of an additive noise that is well mastered in the framework of threshold methods [5]. This approach is not entirely satisfactory, the estimator of the reflectivity obtained is biased and the strong target reflectors are smoothed [6]. In the spirit of the Gamma-MAP filter, a MAP criteria is applied to the domain of the wavelet coefficients. The paper is organized in the following manner : first, the hypotheses and the statistical models of the image are presented (section 2). In section 3, we discuss briefly the wavelet transform algorithm used. In section 4, the introduction of the multiplicative model permits the segmentation of high frequency images into homogeneous, hetereogeneous and highly heterogeneous zones. From gamma distribution hypotheses for speckle and reflectivity, the moments of the wavelet coefficients up to order 4 are expressed explicitly (section 5.2). As a model for the different distributions, we apply the Pearson distribution system leading to a type IV (section 5.2). The Bayesian estimation of the wavelet coefficient of the reflectivity is then the solution of a third-degree equation (section 5.3). The proposed algorithm is tested on a monoview image and the results are compared to the improved Gamma-MAP filter [3].

2. STATISTICAL IMAGE MODEL AND HYPOTHESIS

2.1. Nature and origin of the speckle

Speckle is a typical noise of coherent imagery (sonar, radar, etc.). It results from interference phenomena between elementary backscattering within the resolution cell [7]. The radar image presents a large pixel to pixel variability which limits the performance of classification and target detection algorithms.

2.2. Statistical models of SAR images

2.2.1. Speckle probability density function

In the case of an intensity image, the observed intensity X depending on the random process of the ground reflectivity Y follows a gamma law:

$$P_{X|Y}(x|y) = \frac{L^L}{y^L \Gamma(L)} x^{L-1} e^{-Lx/y}$$

Usually the speckle random process is normalized, which gives a random process Z of mean $E[Z] = \mu_Z = 1$ and the pdf is $\Gamma(L, L)$:

$$P_Z(z) = \frac{L^L}{\Gamma(L)} z^{L-1} e^{-Lz}$$

This normalization leads to the multiplicative model largely employed in the literature:

$$X = YZ \tag{1}$$

Random variables Y and Z are considered to be independent, when the speckle is assumed to be fully developed. The multiplicative model is considered valid within homogeneous and weakly textured areas. The relation (1) leads to the following relation between the different normalized standard deviations of the ground reflectivity, the speckle and the intensity:

$$\mu_X = \mu_Y \mu_Z = \mu_Y \tag{2}$$

$$C_Y^2 = \frac{C_X^2 - C_Z^2}{1 + C_Z^2} \tag{3}$$

with $C_Y = \dfrac{\sigma_Y}{\mu_Y}$, $C_X = \dfrac{\sigma_X}{\mu_X}$, $C_Z = \dfrac{\sigma_Z}{\mu_Z} = \dfrac{1}{\sqrt{L}}$.

2.2.2. Reflectivity and intensity probability density functions

Different distributions are possible for modeling the probability density function of the reflectivity Y. The most widely used is the gamma distribution. Incidentally, it is the basis for the Nezry Gamma-MAP filter [3]:

$$P_Y(y) = \frac{\nu^\nu}{\mu_Y^\nu \Gamma(\nu)} y^{\nu-1} e^{-\nu y/\mu_Y}$$

Where μ_Y is the mean reflectivity in the considered zone, the degree of heterogeneity is measured by $\nu = \frac{\mu_Y^2}{\sigma_Y^2} = 1/C_Y^2$. Presuming a gamma pdf for Y, we obtained a K pdf for the observed intensity which has been proved to be well adapted at describing reality [8].

3. MULTISCALE ANALYSIS

3.1. Principle

Multiresolution analysis permits the analysis of the signal in many frequency bands or at many scales [9]. In practice, multiresolution analysis is carried out using a filter bank composed of a low-pass $\{h_i\}$ and a high-pass $\{g_i\}$ filter. In the case of an image, the filtering is implemented in a separable way by filtering the lines and columns. The low-pass filtering of level j provides an approximation of the initial image at the scale of 2^j. The high-pass filterings give the images of the wavelet coefficients or the high frequency images. The reader can refer to the papers of Mallat [9] and Daubechies [10] for further explanations on multiresolution analysis.

3.2. Stationary wavelet transform

Originally, multiresolution analysis was used for the purpose of signal compression. The wavelet coefficients are sampled based on the Nyquist criteria. The representation is accordingly non redundant and the total number of samples in the representation is equal to the total number of the image pixels. Pyramidal multiresolution analysis is not desirable for estimation/detection problems. The major inconvenience of this representation is that it does not conserve an essential property in image processing, which is the invariance by translation. This property insures that the contours present in the image will be represented on the wavelet levels independently from their position in the image. In order to preserve the invariance by translation, the sub-sampling operation must be suppressed [11], and the decomposition obtained is then redundant[1] and is called a stationary wavelet transform [12] or a “à trous” algorithm [11]. The stationary wavelet transform was used successfully for the noise removal of audio signals [13]. In practice, the structure in cascade of the filter bank does not change; the operations of sub-sampling and over-sampling are simply suppressed. In order to conserve a half-band filtering at each level j, 2^{j-1} zeros are inserted between the coefficients of the low-pass and high-pass filters. We note $\mathbf{W}^{[j,\epsilon]}$, the operator permitting to obtain the wavelet coefficients at scale 2^j (where $\epsilon \in \{h, v, d\}$ designates the horizontal, vertical and diagonal orientations respectively). The image X is thus decomposed into $3J$ high frequency images and one low frequency image:

$$X \leftrightarrow \{\mathbf{A}^{[J]}X, \{\mathbf{W}^{[j,\epsilon]}X,\ 1 \leq j \leq J,\ \epsilon \in \{h, v, d\}\}\}$$

4. HIGH FREQUENCY IMAGE SEGMENTATION

Using the filtering equations, we find a relation equivalent to the relation (3):

$$C_Y^2 = \frac{C_{W_X}^2 - S_2^{[j,\epsilon]} C_Z^2}{S_2^{[j,\epsilon]}(1 + C_Z^2)} \tag{4}$$

with $C_{W_Z} = \sqrt{S_2^{[j,\epsilon]}} C_Z$ et $C_{W_Z} = \sigma_{W_X}/E[X]$; $S_2^{[j,\epsilon]}$ provides the power gain in the filtering process and can be expressed by the relation 11). Using the local estimation of C_{W_X}, this relation permits the segmentation of the high frequency images into homogeneous (where $C_{W_Y} \leq 0$) and heterogeneous (where $C_{W_Y} > 0$) zones. For strong reflectors where the radar response is deterministic, the corresponding wavelet coefficients must be conserved. A high threshold for C_{W_X} derived from the threshold used in the Gamma-MAP filter [3] permits the preservation of these regions:

$$C_{W_X,max} = \sqrt{S_2^{[j,\epsilon]}} \sqrt{1 + 2/L} \tag{5}$$

5. MAP WAVELET COEFFICIENT FILTERING

5.1. Weighting of the wavelet coefficient using a MAP criteria

The filtering equation for obtaining the wavelet coefficients of level j can be rewritten as follows:

[1] All the images obtained conserve the size of the initial image.

$$\begin{aligned} W_X &= \mathbf{W}^{[j,\epsilon]}Y + \mathbf{W}^{[j,\epsilon]}Y(Z-1) \\ &= W_Y + W_B \end{aligned}$$

The pdf of Y depending on the observation X can be expressed using the Bayes relation:

$$P_{W_Y|W_X}(w_Y|w_X) = \frac{P_{W_X|W_Y}(w_X|w_Y)P_{W_Y}(w_Y)}{P_{W_X}(w_X)}$$

The estimate $\hat{w}_Y$ maximizing the *a posteriori* pdf then verifies the following equation:

$$\frac{d\left(ln\left(P_{W_B|W_Y}(w_B|w_Y)\right) + ln\left(P_{W_Y}(w_Y)\right)\right)}{dw_Y}|_{w_Y=\hat{w}_Y} = 0 \qquad (6)$$

In order to apply this Bayesian estimation, we have to establish a model for the different pdf.

5.2. Probability density function of the wavelet coefficient

In the case of a gamma distribution hypothesis for the ground reflectivity and the speckle, we can express the moments of the wavelet coefficients up to order 4. The Pearson distribution system permits modeling using a differential equation, the unimodal pdf $f(x)$ having a tangent contact with the x axis at the extremities. The Pearson coefficients can be expressed simply from the first 4 moments:

$$\begin{aligned} b_1 = a &= -\frac{\mu_3(\mu_4 + 3\mu_2^2)}{A} \\ b_0 &= -\frac{\mu_2(4\mu_2\mu_4 - 3\mu_3^2)}{A} \\ b_2 &= -\frac{(2\mu_2\mu_4 - 3\mu_3^2 - 6\mu_2^3)}{A} \\ A &= 10\mu_2\mu_4 - 18\mu_2^3 - 12\mu_3^2 \end{aligned} \qquad (7)$$

and:

$$\begin{aligned} B_0 &= b_0 + a^2(1+b_2) \\ B_1 &= a(1+2b_2) \\ B_2 &= b_2 \end{aligned} \qquad (8)$$

The type of distribution is indicated by the values $K = B_1^2/(4B_0B_2)$. It can be shown that in the case of a gamma distribution for the gray levels of the original image, the distribution of the wavelet coefficients is Pearson type IV ($0 < K < 1$):

$$f(x) = k\left((x-a+\gamma)^2 + \delta^2\right)^m e^{\left(-\lambda \arctan\frac{x-a+\gamma}{\delta}\right)} \qquad (9)$$

with:

$$m = \frac{1}{2B_2},\ \lambda = \frac{\gamma}{B_2\delta},\ \gamma = \frac{B_1}{2B_2},\ \delta^2 = \tau - \gamma^2,\ \tau = \frac{B_0}{B_2}$$

Using the second moment functions[2] [14] and the linear filtering equations, we can express the first 4 moments of W_Y and W_B.

[2] logarithm of the moment generating function.

$$\begin{aligned} &\mu_{W_Y,1} = 0\,,\ \mu_{W_Y,2} = S_2^{[j,\epsilon]}\frac{\mu_Y^2}{\nu} \\ &\mu_{W_Y,3} = S_3^{[j,\epsilon]}\frac{2\mu_Y^3}{\nu^2}\,,\ \mu_{W_Y,4} = S_4^{[j,\epsilon]}\frac{6\mu_Y^4}{\nu^3} + 3(S_2^{[j,\epsilon]})^2\frac{\mu_Y^4}{\nu^2} \end{aligned}$$

$$\begin{aligned} &\mu_{W_B,1} = 0\,,\ \mu_{W_B,2} = S_2^{[j,\epsilon]}\frac{\mu_Y^2}{L}\left(1+\frac{1}{\nu}\right) \\ &\mu_{W_B,3} = S_3^{[j,\epsilon]}\frac{2\mu_Y^3}{L^2}\left(1+\frac{3}{\nu}+\frac{2}{\nu^2}\right) \\ &\mu_{W_B,4} = S_4^{[j,\epsilon]}\frac{6\mu_Y^4}{L^3}\left(1+\frac{6}{\nu}+\frac{11}{\nu^2}+\frac{6}{\nu^3}\right)(1+L/2) + 3\mu_{W_B,2}^2 \end{aligned}$$

Where $S_n^{[j,\epsilon]}$ can be expressed simply in relation to the filter coefficients.

$$S_n^{[j,\epsilon]} = \left(\sum_k (g_k)^n\right)\left(\sum_l (h_l)^n\right)^{2j-1},\ \epsilon = h, v \qquad (10)$$

$$S_n^{[j,d]} = \left(\sum_k (g_k)^n\right)^2\left(\sum_l (h_l)^n\right)^{2(j-1)} \qquad (11)$$

5.3. Maximum a posteriori equation

Assuming a type IV model for the probability density function of W_Y and W_B, the MAP equation (6) leads to a single point MAP estimate $\hat{w}_Y$ which is the solution of a third degree equation:

$$A_3\hat{w}_Y^3 + A_2\hat{w}_Y^2 + A_1\hat{w}_Y + A_0 = 0 \qquad (12)$$

with:

$$\begin{aligned} A_3 &= B_{B,2} + B_{Y,2} \\ A_2 &= -B_{B,2}(2U_B + V_Y) - B_{Y,2}(2U_Y + V_B) \\ A_1 &= B_{B,2}(U_B(U_B + 2V_Y) + \delta_B^2) \\ &\quad + B_{Y,2}(U_Y(U_Y + 2V_B) + \delta_Y^2) \\ A_0 &= -B_{B,2}V_Y(U_B^2 + \delta_B^2) - B_{Y,2}V_B(U_Y^2 + \delta_Y^2) \end{aligned} \qquad (13)$$

$$\begin{aligned} U_B &= w_X - a_B + \gamma_B \\ V_B &= w_X - a_B \\ U_Y &= a_Y - \gamma_Y \\ V_Y &= a_Y \end{aligned} \qquad (14)$$

6. RESULTS AND CONCLUSION

The image is at first decomposed into $3J$ high frequency images. Each high frequency image is segmented according to the procedure described in section 4. The wavelet coefficients of the homogeneous zones are set at zero, equation (12) is applied in the heterogeneous zones while those in the highly heterogeneous zones are conserved. Then, the filtered image is obtained by reconstruction from the high frequency images filtered accordingly. Figure 2 shows the result of the proposed filtering for the Figure 1 image ($J = 3$, bi-orthogonal wavelets [10]). The classical Gamma-MAP filter is provided for comparison purposes in Figure 3. Multiscale filtering appears to better preserve details, in particular in the homogeneous areas for a same degree of smoothing.

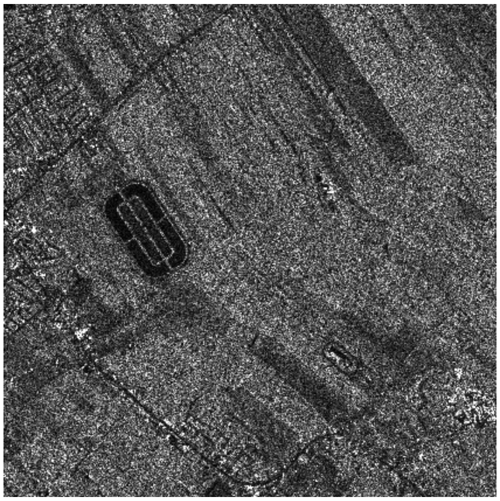

Figure 1: Original image (RADARSAT, one look)

Figure 2: Proposed filter with bi-orthogonal wavelets (5 coefficients)

Figure 3: Gamma-MAP filter

7. REFERENCES

[1] Lee J.S., "A simple speckle filtering algorithm for synthetic aperture radar images," *IEEE Trans. SP*, vol. 13, no. 1, pp. 85–88, January 1983.

[2] D.T. Kuan, A.A. Sawchuk, T.C. Strand, and P. Chavel, "Adaptative restoration of images with speckle," *IEEE Trans. ASSP*, vol. 35, no. 3, pp. 373–383, March 1987.

[3] A. Lopes, E. Nezry, and H. Laur, "Structure detection and statistical adaptive speckle filtering in sar images," *International Journal of Remote Sensing*, vol. 14, no. 9, pp. 1735–1758, 1993.

[4] T. Ranchin, *Applications de la transformée en ondelettes et de l'analyse multirésolution au traitement des images de télédétection*, Ph.D. thesis, Université de Nice-Sophia Antipolis, Nice, France, July 1993.

[5] D.L. Donoho and I.M. Johnstone, "Adapting to unknown smoothness via wavelet shrinkage," *Journal of the American Statistical Association*, vol. 90, no. 432, pp. 1200–1224, December 1995.

[6] R. Touzi, *Analyse d'images radar en télédétection: améliorations radiométriques, filtrage du speckle et détection des contours*, Ph.D. thesis, Université Paul Sabatier, Toulouse, France, 1988.

[7] F.T. Ulaby, F. Kouyate, Brisco B., and T.H. LEE Williams, "Textural information in sar images," *IEEE Trans. GRS*, vol. 24, no. 2, pp. 235–245, March 1986.

[8] C.J. Oliver, "Information from sar images," *J. Phys. D: Applied Physics*, vol. 24, no. 6, pp. 1493–1514, 1991.

[9] S. Mallat, "A theory for multiresolution signal decomposition: The wavelet representation," *IEEE Trans. PAMI*, vol. 11, no. 7, pp. 674–693, July 1989.

[10] I. Daubechies, *Ten lectures on wavelets*, SIAM, 1992.

[11] M.J. Shensha, "The discrete wavelet transform: Wedding the a trous and mallat algorithms," *IEEE Trans. SP*, vol. 40, no. 10, pp. 2464–2482, October 1992.

[12] G.P. Nason and B.W. Silverman, "The stationary wavelet transform and some statistical applications," Tech. Rep., Department of Mathematics, University of Bristol, Bristol, BS8 1TW, 1995.

[13] D.P. Pesquet, "Time-invariant orthonormal wavelet representations," *IEEE Trans. SP*, vol. 44, no. 8, pp. 1965–70, August 1996.

[14] A. Papoulis, *Probability, Random variables, and Stochastic Processes*, Mc Graw-Hill, 3 edition, 1991.